Spectroscopic investigation of fluctuating anisotropic electric fields in a high-power-diode plasma

E. Sarid,* Y. Maron, and L. Troyansky
Department of Physics, Weizmann Institute of Science, Rehovot 76100, Israel
(Received 11 September 1992)

Fluctuating anisotropic electric fields in the anode plasma of a high-power ion diode are investigated as a function of time throughout the 100-ns-long voltage pulse by polarization spectroscopy of hydrogen lines. The H_α and H_β spectral profiles observed for different polarizations and lines of sight are compared to calculations, based on the quasistatic approximation, of the emission pattern resulting from the combined influence of the ionic and the turbulent electric fields. Assuming one-dimensional Rayleigh distributions for the turbulent field amplitudes, the difference between the linewidths observed for orthogonal polarizations yields mean amplitudes $\gtrsim 5$ kV/cm for the turbulent fields. Furthermore, accounting for the effect of the anisotropic fields on the spectral line profiles allows for a downward correction of the electron density obtained from the width of the Stark-broadened H_β line by a factor of $\simeq 2$. This in turn leads to a higher estimate of the electron temperature obtained from observed line intensity ratios and use of time-dependent collisional-radiative calculations.

PACS number(s): 52.70.Kz, 52.25.Gj, 52.25.Rv

I. INTRODUCTION

Turbulence occurs commonly in plasmas, both in space and in laboratory devices. In general, its source is lack of thermodynamic equilibrium in the plasma; it can be driven by the non-Maxwellian character of the plasma constituent distribution or by spatial inhomogeneities [1–3]. The turbulence gives rise to electric and magnetic fluctuations which can affect stability as well as transport and heating processes. Determining its source and mechanism can be thus crucial for understanding the observed plasma behavior and for placing limits on the performance of plasma devices [4,5]. In intense ion-beam diodes that are considered in this paper the turbulence has been previously conjectured [6–8] to be the source of anomalous resistivity that causes the observed rapid plasma expansion and a fast magnetic-field penetration as well as produces the flat temperature profile. It has been shown that the experimental observations can be explained by an anomalous resistivity about ten times larger than the classical value. A possible source of the resistivity anomaly is turbulent electric fields that enhances the effective collision rate of plasma electrons.

In addition to the above-mentioned phenomena, turbulent electric fields can, as pointed out by Nee and Griem [9], significantly influence the spectral emission line profiles in the plasma. Consequently, the determination of plasma density from Stark-broadening data is affected. Furthermore, since in non-LTE (LTE denotes local thermal equilibrium) plasmas determination of the electron temperature from line-intensity ratios is dependent on the electron density assumed, better determination of the electron density improves the determination of the electron temperature.

Turbulence in plasma can be investigated by studying the fluctuations of plasma parameters such as the electron density or temperature, or by measuring the fluctuations in the electric or magnetic fields [10]. In this study, we utilize polarization measurements of the Stark broadening of hydrogen lines [11] to determine, in the 100-ns time scale, the amplitude and direction of turbulent electric fields in the anode plasmas in a magnetically insulated intense ion diode.

The diagnostic method is based on the different Stark-splitting and polarization properties of the σ ($\Delta m = \pm 1$) and the π ($\Delta m = 0$) components of the hydrogen lines. Under the influence of a static (or quasistatic) electric field, the π components have larger Stark shifts than the σ components. Thus, if the electric fields in the plasma have a preferred direction in space, the widths of the hydrogen emission lines observed for a polarization parallel to the fields (for which the π components are predominant) are larger that those observed for a polarization normal to the fields (for which the σ components are predominant).

Polarization spectroscopy has been used for the observation of fluctuating anisotropic electric fields in various plasma devices on time scales longer than that of the present experiment. It was first used by Zavoiskii *et al* [12] to measure fields in a direct-discharge plasma in a mirror machine. Anisotropic fields of about 30 kV/cm were found and were associated with ion-acoustic oscillations in the direction of the discharge current. The method has been applied also to the rf discharge plasma [13], to a mirror machine with opposite-sign magnetic fields [14], to the Θ pinch [15], to the Z pinch [16], and more recently also to the edge plasma of the T-10 tokamak [17]. Use of this method was suggested for the investigation of turbulence in solar flares [18]. Spectroscopic investigations of electric fields due to plasma instabilities using observations of various aspects of the Stark effect have been discussed by Griem [19], and by Bekefi, Deutsch and Yaakobi [20].

Inferring the anisotropic field properties from anisotropic Stark-broadening data requires the calculation of the spectral line broadening under the combined

influence of turbulent fields and plasma particle fields. In previous experiments [12–17], the plasma particle fields were much lower than the observed anisotropic fields and were neglected. Oks and Sholin [21] analyzed the spectral profiles under the influence of both the particle and turbulent fields but assumed an isotropic turbulent spectrum. In the present study, we assume a one-dimensional (1D) Gaussian turbulent field distribution and obtain the total electric-field distribution by convolution with the isotropic Holtzmark field in the plasma. The emission pattern is then calculated for the line of sight perpendicular to the turbulent field direction. The calculated pattern for each of the orthogonal polarizations was compared to the spectral profiles observed for the two polarizations and for the two orthogonal lines of sight to obtain the amplitude and direction of the turbulent fields.

The turbulent fields observed in our planar anode plasma were found to point mainly perpendicular to the anode surface. Their amplitude was found to be a few kV/cm comparable to or larger than the amplitude of the plasma particle fields (the Holtzmark field) and to decrease in time during the pulse. The anisotropy of the fields is presumably related to the direction of the particle flows in the anode plasma which serve as the source of the free energy. Litwin, Sarid, and Maron [22] have recently suggested that a modified two-stream instability, resulting from the ion drift [6] through the magnetized electron background in the plasma, is the most likely to be responsible for the turbulent electric fields observed here. Comparison of the model predictions of the amplitude, direction, and frequency range of the saturated electric fields with the experimental results will be given separately.

Hydrogen line profiles have often been used to determine the plasma density, in particular in ion diodes [23,6,24]. However, possible effects of turbulent fields on the determination of the density have generally been ignored. If the turbulent electric fields are comparable to the particle fields in the plasma they significantly increase the line Stark broadening. Thus, neglecting the effect of the turbulent fields leads to an overestimate of the plasma density. In our previous experiment [6], using the width of the Stark-broadened H_β line, the plasma density was determined to be $\simeq 2.2\times 10^{15}$ cm^{-3}. In the present study, accounting for the turbulent field effect on the emission profile suggests that the plasma density is lower by a factor $\lesssim 2$. Furthermore, since our electron density is used to determine the electron temperature in this nonequilibrium anode plasma, this smaller electron density enables us to correct our previously determined electron temperature [8] from 5–8 eV to 10±3 eV.

II. EXPERIMENTAL ARRANGEMENT

The anode plasma investigated in these experiments is produced via a surface flashover of a dielectric sheet that serves as the anode in the planar magnetically insulated diode described in Ref. [6]. In brief, the diode, shown in Fig. 1(a), is powered by a 270-kV, 90-ns pulse delivered by an LC generator coupled to a 1-Ω water line. The insulating magnetic field B_z is 6 kG, and is applied parallel to the anode surface in order to inhibit the electron flow across the diode gap. The dielectric anode sheet over which the plasma is formed, called here the active anode, was made of epoxy that filled grooves in the z direction in an aluminum plate, see Fig. 1(b). The height in the y direction of the active anode was 6 cm and the length in the z direction was either 2 or 8 cm. Using both the 2-cm- and the 8-cm-long anodes enabled us to examine possible effects of self-absorption and edge effects on the data (see below). The anode-cathode gap was 0.8 cm. Typical wave forms of the diode voltage and current are shown in Figs. 2(a) and 2(b).

The diagnostic system is shown in Fig. 3. Light was collected from the anode plasma and directed onto the spectrometer input slit using the demagnifying lens L. The distance of the observed plasma region from the anode surface was varied by moving the mirror M normal to the anode. The spatial resolution normal to the anode was determined by the width of the spectrograph input slit by the demagnification of the imaging lens L and by the length of the active anode.

In order to observe the spectral line profile in a single

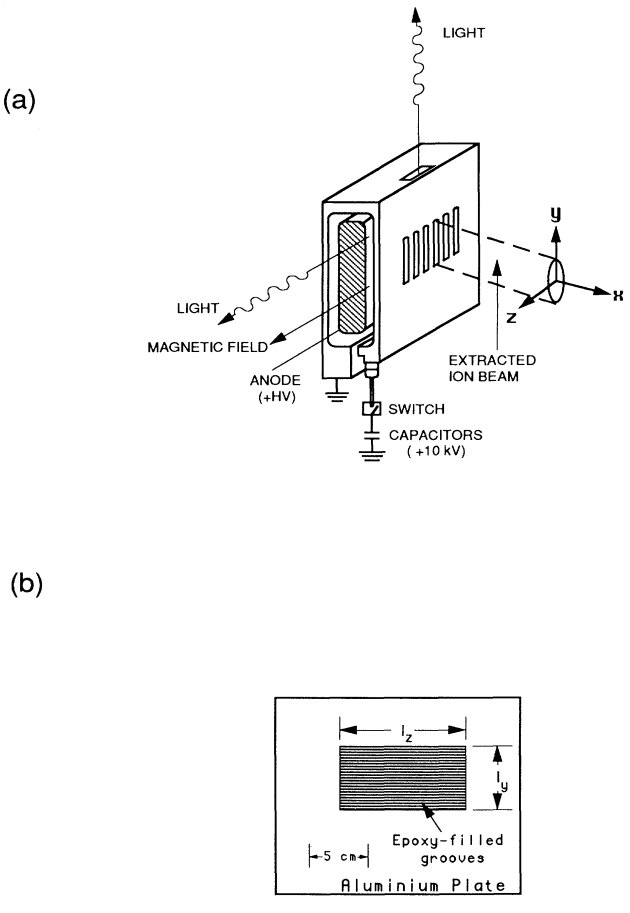

FIG. 1. (a) Schematic illustration of the planar magnetically insulated diode. The arrows that show directions of light emission denote the two lines of sight used in the present experiments. (b) A view of the anode showing the active anode geometry. The active anode length and height are l_z and l_y, respectively. l_y used was 6 cm and l_z was either 2 or 8 cm.

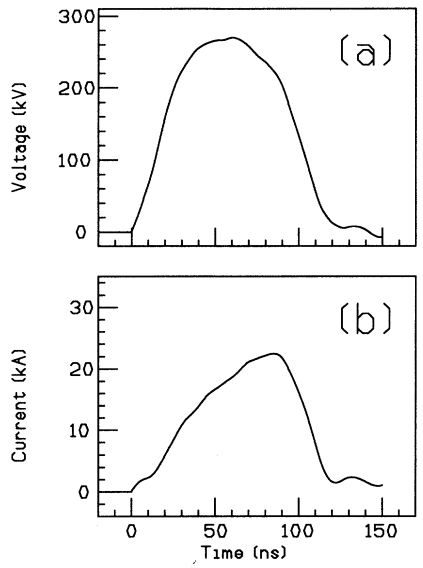

FIG. 2. (a) Diode voltage for $B_z=6$ kG; (b) diode total current.

discharge the light at the spectrograph output window was further dispersed using the cylindrical lens CL (see Fig. 3) and projected onto a rectangular array of 11 fiber bundles. Each bundle was 0.3-mm wide and 20-mm high. Using the lens CL the spectral dispersion was varied in the experiments between 0.23 to 1.05 Å per bundle. These values also determined the spectral resolution.

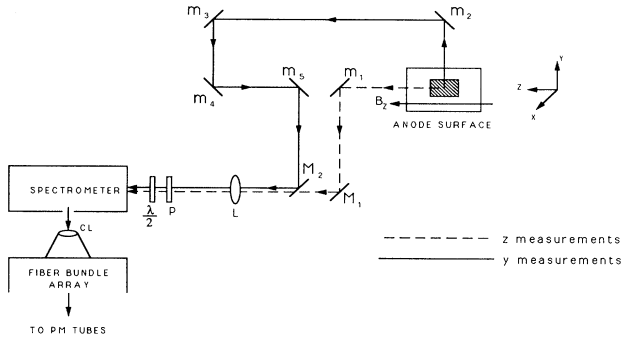

FIG. 3. Experimental system used for the polarization spectroscopy. The lines of sight were parallel to the anode surface. In the z measurements light is collected in the z direction and is directed onto the spectrograph by the mirrors m_1 and M_1 and the lens L. In the y measurements light is collected in the y direction with the aid of the mirrors m_2, m_3, m_4, m_5, and M_2 and the lens L. The polarizer P selects the axis of the observed polarization, and the $\lambda/2$ plate rotates the axis to the higher-sensitivity direction of the spectrograph. A cylindrical lens CL is used to disperse the light at the spectrograph output and to project it onto a rectangular fiber-bundle array composed of 11 bundles, each of which transmits the light to a fast photomultiplier tube. The spectral line profile is thus measured as a function of time in a single discharge. The direction perpendicular to the anode is denoted by x, and the applied magnetic field B_z is in the z direction. The hatched region indicates the active-anode region.

Each fiber bundle transmitted the light signal to a photomultiplier tube, the signal of which was recorded by a digital oscilloscope. Thus, 11 points of the spectral profile were obtained in a single discharge. The spectral channels were calibrated with respect to each other over the entire usable spectrum.

Measurements were performed for lines of sight in the z and y directions, denoted here as the z measurements and y measurements, respectively. For the z measurements we observed the line emission polarized either in the x or y directions and for the y measurements polarizations in the x and z directions were selected. The polarization of the line emission collected by the spectrograph was set by the linear polarizer P, see Fig. 3.

Because of the dependence of the spectrograph grating efficiency on the light polarization, the diffraction efficiency for the H_α line (6563 Å) for the polarization parallel to the grating grooves is $\simeq 10\times$ lower than for the orthogonal polarization. In order to obtain higher efficiency for the polarization parallel to the grooves (corresponding to the y or the z polarizations in the z and the y measurements, respectively), a $\lambda/2$ plate (see Fig. 3) was used to rotate this polarization to the direction perpendicular to the grooves. The $\lambda/2$ plate was always used, even in the experiments in which it was not used to rotate the polarization, in order to avoid differences between the optical systems used for the various measurements. It was verified that the intensity of measured lines was identical for the two combinations of the polarizer and the $\lambda/2$ plate polarization perpendicular to the grooves and no rotation by the plate, or polarization parallel to the grooves and a 90° rotation by the plate.

Using a calibration lamp mounted in the diode and an additional polarizer it was also verified that none of the optical components apart from the polarizer P and the $\lambda/2$ plate affected the polarization of the light emitted from the diode region. Furthermore, the change in the distance from the anode surface of the plasma region viewed by the spectroscopic system, caused by the rotations of polarizer and the $\lambda/2$ plate as a result of unparallel faces of one of the components, was found to be less than 0.1 mm. It was corrected by moving the 45° mirror (mirrors M_1 or M_2 in Fig. 3, depending on the line of sight used).

III. EXPERIMENTAL RESULTS

Several series of experiments were performed to obtain the profiles of the hydrogen lines for the orthogonal polarization directions x, y, and z. In all experiments the widths of H_α and H_β polarized in the x direction were found to be larger than of those polarized in the y or z directions. In this section we present the measured width differences. The inferred magnitude of the anisotropic electric fields in the plasma is discussed in Sec. IV.

A. H_α line

The H_α profile is dominated by the presence of an unshifted central component as can be seen in the Stark-splitting pattern shown in Fig. 4. In the presence of one-

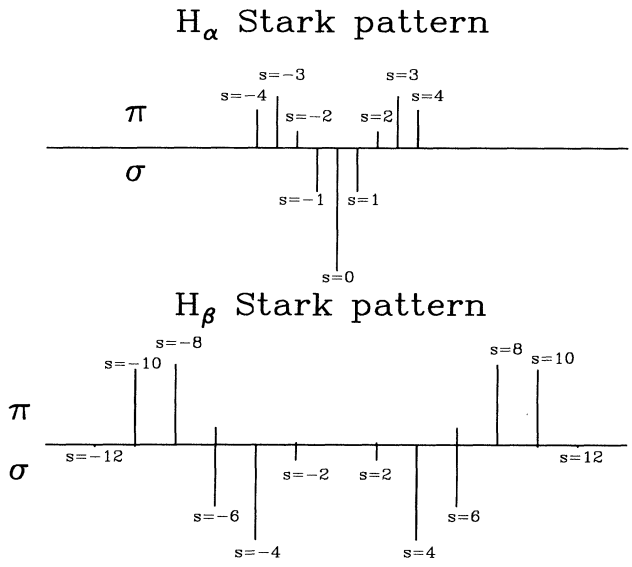

FIG. 4. Stark-splitting patterns of H_α and the H_β under a static electric field. The splitting parameter s is $s=n(k_1-k_2)-n'(k_1'-k_2')$, where n and n' are the principle quantum numbers of the upper and lower level of the transitions, respectively. k_1 and k_2 (k_1' and k_2') are the parabolic quantum numbers of the upper (lower) levels. For each line the π ($\Delta m=0$) and the σ components ($\Delta m=\pm 1$) are shown as positive and negative components, respectively. The amplitudes of the components represent their relative intensities.

dimensional electric fields, this component is absent if the line of sight is perpendicular and the polarization is parallel to the field. Therefore, the observed profile is much wider for the line polarized in the direction of the field than for that polarized perpendicular to it. In the presence of anisotropic fields that are not one dimensional, the line is expected to be wider for a polarization parallel to the stronger component of the field.

The spectral dispersion used for the observations of the H_α spectral profiles was 0.76 Å per channel, which allowed for recording the entire line profile in a single discharge. Examples of profiles for orthogonal polarizations in the y measurements showing a wider profile for the x polarization are shown in Fig. 5.

The widths obtained for various polarizations in the z and the y measurements are given as a function of time in Fig. 6. The experiments were performed with a 2-cm-long anode. The spatial resolution in the x direction was 0.5 mm for the z measurements and 0.8 mm for the y measurements. The distance of the region viewed from the anode surface was varied in the experiments and the data presented in Fig. 6 are averaged over the different locations in the range $x=0-1.5$ mm. For each x a pair of discharges was performed using orthogonal polarizations.

For both lines of sight H_α was found to be wider for the polarization in the x direction than for the orthogonal (y or z) polarizations. Significant differences in the widths for the two polarizations are seen for $t=40-90$

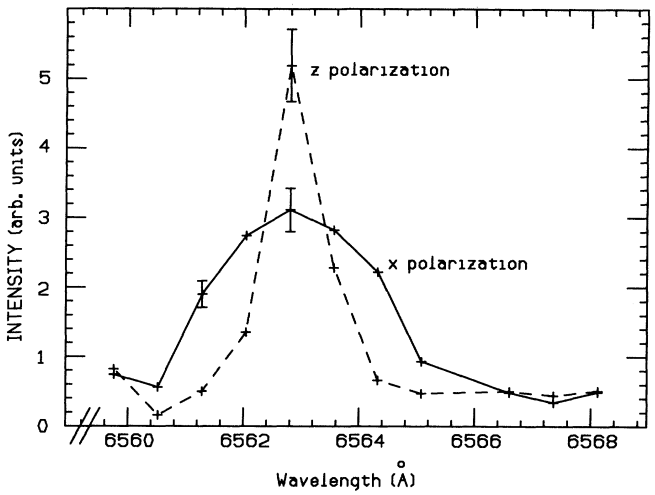

FIG. 5. Measured profiles of the H_α line observed using a line of sight in the y direction (a y measurement). The spectral resolution is 0.76 Å per channel. The solid line is the profile obtained for polarization in the x direction, and the dashed line for polarization in the z direction. The data points are connected by straight lines.

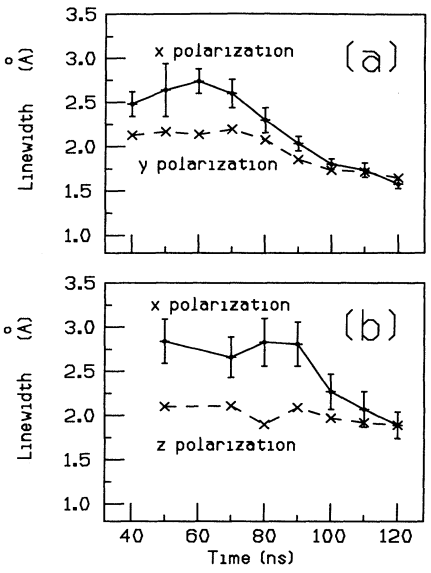

FIG. 6. H_α FWHM as a function of time observed with a 2-cm-long anode. $t=0$ is the time of the start of the diode voltage pulse. The data are averaged over the different locations in the range $x=0-1.5$ mm. The error bars indicated were obtained by dividing the standard deviation of the measured width differences (obtained for each x) by $\sqrt{N-1}$, where N is the number of discharges for each polarization. Thus, they represent error bars on the difference between the two curves. (a) The line of sight is in the z direction and widths for polarizations in the x and y directions are given by the solid and dashed curves, respectively. Each curve is an average over seven discharges. (b) The line of sight is in the y direction and widths for polarizations in the x and z directions are given by the solid and dashed curves, respectively. Each curve is an an average over nine discharges.

ns, followed by a decrease in the differences until they vanish at $t \simeq 120$ ns. At $t = 50-70$ ns, the measured widths were very similar for the two liens of sight. In the z measurement, the spatially averaged widths were found to be 2.66 and 2.17 Å for the x polarization and y polarization, respectively, and in the y measurements 2.67 and 2.10 Å for the x polarization and z polarization, respectively.

The only significant difference between the results for the two lines of sight was the increase in the width difference at $t = 80-90$ ns in the y measurements, mainly caused by the large width difference observed at $x = 0.5-1$ mm. These large differences in the widths at $x = 0.5-1$ mm and $t = 80-90$ ns found for the 2-cm-long anode were also observed for the 8-cm-long anode as can be seen in Table I, where the results are given for $t = 80-130$ ns. The data presented are averages over groups of five to seven discharges for which plasma regions between $x = 0.5$ to 1 mm were observed. For both anodes, differences of about 1 Å between the widths for the x and z polarizations are observed at $t = 80-90$ ns, decreasing significantly in the following 20 ns. For $t = 110-130$ ns the differences between the two orthogonal polarizations are small.

The similarity of the results of the y measurements for the two lengths of the active anode indicate that edge effects due to the finite anode length do not affect the H_α width significantly. Also, since different epoxy admixtures were used for these two anodes (in the 8-cm-long anode experiments pure epoxy was used, while in the 2-cm-long anode experiments the epoxy was mixed with MgF_2, CaF_2, and $AlNaSiO_3$, each constituting 20% by weight of the entire mixture, similar to the earlier experiments described in Refs. [6–8,25], it appears that the H_α width was unaffected by the epoxy admixture used.

The results of the z measurements for $x > 0.5$ mm were also found to be similar for the 2-cm-long and the 8-cm-long active anodes. However, for $x = 0-0.5$ mm, the H_α widths observed for both polarizations were found to be larger for the longer anode than those of the shorter one. Since the hydrogen density is larger near the anode surface [25], it is possible that the increase in the H_α width seen near the long anode is caused by self-absorption along the long light path in the plasma. This suggestion is supported by measurements of resonant laser absorption by hydrogen atoms in the anode plasma [26]. The similarity of the results for $x > 0.5$ mm for all experiments, as well as for $x < 0.5$ mm for all z and y measurements except of the z measurements with the 8-cm-long anode, strongly indicates that the effect of self-absorption on these results is small.

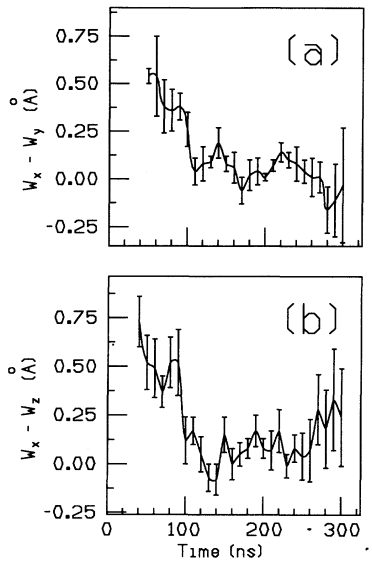

FIG. 7. Differences between the H_α widths observed for the two orthogonal polarizations. The anode length was 8 cm. (a) The line of sight is in the z direction. W_x and W_y are the widths for the polarizations in the x and y directions, respectively. The data points are an average over ten discharges (five for each polarization) performed with $x = 0.5-1.5$ mm. (b) The line of sight is in the y direction. W_x and W_z are the widths for the x and z polarizations, respectively. Here, each data point is an average over 38 discharges (19 for each polarization) performed with $x = 0-1.5$ mm.

The differences in the linewidths for the orthogonal polarizations obtained with the 8-cm-long anode are shown in Fig. 7. Figure 7(a) shows the time dependence of the difference between the width for the x polarization (W_x) and that for the y polarization (W_y) observed in z measurements. Here, only the results for $x > 0.5$ mm were

TABLE I. FWHM of the H_α line observed in the y direction for polarizations in the x and z directions. For the 2-cm-long anode and for the 8-cm-long anode each width is an average of five discharges and seven discharges, respectively. For all discharges x was between 0.5 to 1 mm.

	H_α FWHM (Å)			
Time	2-cm-long active anode		8-cm-long active anode	
(ns)	x polarization	z polarization	x polarization	z polarization
80	3.07±0.33	1.49±0.09	2.90±0.24	2.24±0.25
90	2.45±0.27	1.54±0.04	2.72±0.17	1.75±0.15
100	1.96±0.25	1.64±0.09	1.98±0.12	1.63±0.06
110	1.77±0.26	1.62±0.13	1.75±0.12	1.69±0.10
120	1.67±0.17	1.66±0.09	1.70±0.14	1.57±0.06
130	1.82±0.08	1.81±0.17	1.76±0.10	1.67±0.14

used in order to avoid possible effects of self-absorption (including the results for $x < 0.5$ mm, however, does not change the spatially averaged widths significantly). Similarly, the difference in the widths $W_x - W_z$ (W_z being the width for the z polarization) observed in the y measurements is given in Fig. 7(b). Here the widths are averaged over $x = 0-1.5$ mm from the anode surface. For both measurements the differences in the width are seen to decrease in time during the voltage pulse and are very small at $t > 100$ ns. Figure 7 also shows the differences later in time after the main voltage pulse. The width differences at later times are much smaller than those seen during the main voltage pulse.

B. H_β line

Due the larger Stark shifts of the π components relative to the σ components, the H_β width is expected to exhibit a dependence on the polarization similar to that of the H_α line even though it lacks an unshifted central component (see Fig. 4). The spectral profile of the H_β line was observed with a spectral dispersion of 1.05 Å per channel in order to obtain the entire profile in a single discharge. The relative errors in the data points for the H_β spectral profiles were larger than those for H_α. This resulted from the lower intensity of H_β and from the shot-to-shot irreproducibility. The irreproducibility probably affected H_β more than H_α because of the dominance of the H_β profiles by the Stark broadening (for all polarizations), which makes these profiles more susceptible to irreproducibility in the electron density. The results for the H_β were therefore averaged over time intervals of 20–50 ns in order to obtain statistically significant results.

H_β widths were observed for the region $x = 0$ to 0.5 mm from the anode surface in three measurement series: 10 measurements in the z direction using a 2-cm-long anode, 14 measurements in the z direction using an 8-cm-long anode, and 8 measurements in the y direction using an 8-cm-long anode. Results are discussed here only for $x = 0-0.5$ mm since statistically significant data were obtained in all series of measurements only for this region. The differences between the widths obtained in each series for the different polarizations are summarized in Fig. 8.

The H_β widths observed in the z measurements with a 2-cm-long anode averaged over the time interval 50–70 ns were 4.20 and 3.59 Å for the x and y polarizations, respectively, the difference being 0.61 ± 0.17 Å as shown in Fig. 8 (for the same region, the corresponding H_α widths were 2.6 and 2.3 Å, with a difference of 0.30 ± 0.10 Å). Similar to H_α, the widths for the two polarizations became about equal for $t > 90$ ms. The width difference averaged over $t = 100-150$ ns was 0.02 ± 0.27 Å.

Qualitatively, similar findings were seen using the 8-cm-long active anode. Unlike H_α, the width of H_β and the differences in the widths for the orthogonal polarizations were smaller for the 8-cm-long anode than those obtained using the 2-cm-long anode. Averaging over $t = 30-80$ ns gave widths $W_x = 3.14$ and $W_y = 2.84$ Å, the width difference being 0.30 ± 0.08 Å. A similar averaging for the y measurements with the same anode gave $W_x = 2.88$ Å and $W_x = 2.64$ Å, the width difference being $0.24 \pm .07$ Å. For both measurements the differences were small for $t > 90$ ns. Averaging over the time interval 90–130 ns yielded $W_x - W_y = -0.01 \pm .07$ Å for the z measurements and $W_x - W_z = 0.04 \pm 0.15$ Å for the y measurements, see Fig. 8.

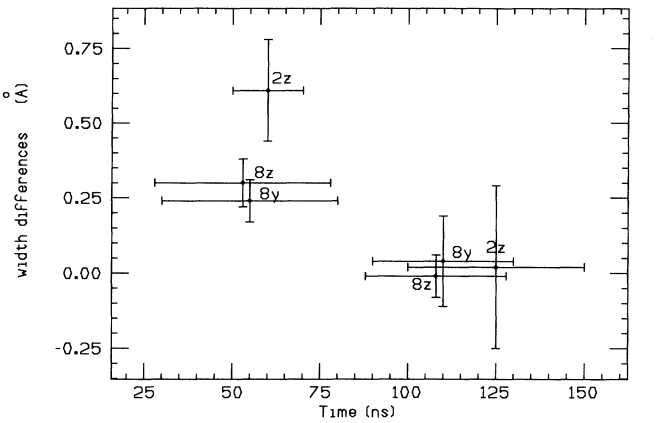

FIG. 8. Results of three series of H_β width measurements. The z measurements are marked by $2z$ and $8z$ for the 2-cm- and 8-cm-long anodes, respectively. For these measurements the width differences between the x and y polarizations $W_x - W_y$ are shown. The points marked by $8y$ show the width differences between the x and the z polarizations $W_x - W_z$ obtained in the y measurements with the 8-cm-long anode. Averages over 10, 14, and 8 discharges were performed to obtain the $2z$, $8z$, and $8y$ points, respectively. x is 0–0.5 mm for all measurements. The horizontal error bars indicate the time intervals over which the results were averaged.

To summarize the results for H_β, the width for the x polarization in the period 30 to 90 s, for the two lines of sight and for two anodes, was observed to be larger than for the other two orthogonal polarizations. For $t > 100$ ns the width differences for the various polarizations were very small.

The dependence of the H_γ profile on the polarization direction was also observed and found to be qualitatively similar to those of H_α and H_β. However, the low H_γ intensity and the nearby presence of impurity lines prevented quantitative analysis. Similar reasons made it impossible to study the H_δ and the H_ϵ profiles.

C. Li *I* 6708-Å line

Polarization measurements similar to those performed for the hydrogen lines were also made for the Li *I* 6708-Å line. The purpose of these measurements was to demonstrate that spectral profiles that are expected to be unaffected by electric fields in the plasma do not depend on the polarization observed.

The effect of electric fields here considered on the Li *I* 6708-Å line profile is negligible since both the upper and lower levels of the $2p \rightarrow 2s$ transition are isolated. The full width at half maximum (FWHM) Stark broadening

at a plasma density of 10^{16} cm^{-3} is 0.02–0.04 Å [27]. In our experiments, the Li *I* 6708-Å line profile is dominated by Doppler broadening. Based on the kinetic energies of $\simeq 8$ eV observed for other neutral atoms in our plasma [6], the line FWHM due to the Doppler broadening is expected to be $\simeq 0.5$ Å. Additional contributions to the line profile are the Zeeman splitting under the applied 6-kG magnetic field ($\simeq 0.3$ Å) and the fine splitting ($\simeq 0.15$ Å).

Since the relative effect of the Zeeman splitting on the line profile is larger for this Li *I* line than for the hydrogen lines, polarization measurements for the Li *I* line can be more affected by the Zeeman-splitting emission properties. However, for the line of sight in the direction of the magnetic field (z axis) as used in our measurements for Li *I*, the σ components are circularly polarized and the Zeeman splitting seen is independent of the linear polarization used for the observation. Note also that the Li *I* line was a convenient line for such a comparison experiment. Having a similar wavelength to H_α, the performance of the optical components, in particular the sensitivity of the spectrograph for the two polarization directions, is very similar to those for H_α.

As for H_α, the Li *I* width for each polarization was obtained by averaging over a few measurements. No dependence of the Li *I* width on the polarization direction was found. For example, for $t = 40$–50 ns the average measured linewidths for the two orthogonal polarizations were 0.65 ± 0.01 Å and 0.66 ± 0.01 Å, respectively (at this time, the difference between the H_α widths for the two orthogonal polarizations was more than 0.5 Å, see above).

The width of 0.65 Å observed for the Li *I* line is estimated to result from Doppler broadening corresponding to a temperature of 6.5 ± 1.5 eV for the lithium atoms (consistent with previous measurements [6]), and the smaller contributions of the Zeeman and the fine splittings. As noted above, the broadening mechanisms of the Li *I* 6708-Å line could not contribute to a dependence of the profiles on the polarization. The observed absence of such a dependence does, therefore, support the claim that the polarization dependence observed for the hydrogen spectral profiles results from the effect of anisotropic electric fields in the plasma.

IV. ANALYSIS OF THE RESULTS

A. Method

In this section we use the dependence of the hydrogen linewidths on the emission polarization to obtain an estimate of the anisotropic electric fields in the plasma. The data given above are analyzed assuming the quasistatic approximation for the anisotropic electric fields in the plasma. This approximation is valid when the field changes on a time scale long compared to that required to affect the optical coherence of the radiation transition. For the hydrogen lines in our plasma it is estimated that field frequencies up to $\sim 10^{11}$ rad/s can be treated under this approximation [28]. In our analysis we calculate the effect of both the anisotropic fields and the quasistatic ionic fields in the plasma on the hydrogen-line emission pattern. The previous analyses known to us either neglected the ionic fields [11–17] or treated only the case of isotropic turbulent fields [21].

The similarity of the width observed in the z and the y measurements discussed above indicates similar electric fields in these directions. The wider lines observed for the x polarization indicate that the anisotropic electric fields mainly point in the x direction. From the excess width for the x polarization the amplitude of the anisotropic fields can be estimated. A Stark width of a few Å of H_β correspond to quasistatic electric fields of a few kV/cm. Anisotropic electric fields that cause a change of the width of H_β from 3.6 to 4.2 Å, see Sec. III, are expected to be of the same order of magnitude.

Motivated by these observations we consider a one-dimensional distribution in the x direction for the anisotropic electric fields in addition to the isotropic particle electric fields in the plasma. Therefore, an axially symmetric distribution function for the convoluted electric fields is constructed, with the x direction as the symmetry axis. Sholin and Oks [11] analyzed a similar situation of an axially symmetric distribution of quasistatic turbulent electric fields, but neglected the isotropic fields. However, the mathematical analysis that follows is similar to theirs.

The Doppler broadening is included in the calculation of the line profiles while the contributions of the Zeeman splitting and the impact broadening, estimated to be <0.3 Å for H_α, are neglected. The contribution of ion dynamic effects [29] can be more significant in the case of H_α (up to 0.8 Å for a plasma density of 2×10^{15} cm^{-3}), although it is smaller than the Doppler contribution. Since the ion dynamic effects are neglected in the present discussion, the Doppler broadenings here obtained yield an upper limit for the hydrogen velocities.

The axially symmetric distribution function for the electric fields in the plasma can be characterized by $W(\mathcal{E},\cos\theta)$, a normalized probability for an electric field of magnitude $\mathcal{E}$ pointing at an angle θ with respect to the symmetry axis (x direction). The emission profiles calculated for the lines of sight in the z and y directions are

$$S_i(\lambda-\lambda_0)=\sum_{s,\nu} I_{s,\nu}\int_{-\infty}^{\infty} M(v)dv \int_0^{\infty} d\mathcal{E} \int_{-1}^{+1} d(\cos\theta) W(\mathcal{E},\cos\theta) f_{i,\nu}(\cos\theta)\delta(\lambda-\lambda_0-\mathcal{E}\Delta_{s,\nu}-vD)\ , \tag{1}$$

where $\lambda-\lambda_0$ is the wavelength displacement from the line center. The index $i=1,2$ corresponds to the direction of the observed polarization. The index $\nu=\pi,\sigma$ refers to the line π or the σ components, while the sum over s is the sum over the Stark components with the splitting parameter s. The integral is a convolution of the Stark pattern of components with amplitudes $I_{s,\nu}$ and Stark shifts $\mathcal{E}\Delta_{s,\nu}$ due to electric fields with the distribution function

$W(\mathcal{E},\cos\theta)$, with the Doppler broadening that results from the velocity distribution $M(v)$ of the hydrogen atoms.

The velocity distribution function $M(v)$ is taken to be a normalized Gaussian distribution in accordance with measurements of velocity distributions for other species in the plasma [6]. This assumption is also consistent with the H_α profiles observed for the polarizations in the y or the z directions (presumably dominated by the Doppler effect, see below). The term vD appearing in the argument of the δ function is the Doppler shift resulting from a velocity v along the line of sight, i.e., $vD=\lambda_0(v/c)$. The Stark shift $\Delta_{s,\nu}\mathcal{E}$ of the s component is given by

$$\Delta_{s,\nu}\mathcal{E}=\frac{3ea_0\lambda_0^2}{2hc}s\mathcal{E} \ . \tag{2}$$

The functions $f_{i,\nu}(\cos\theta)$ describe the angular dependence of the intensity of the observed Stark components. The projections of the π and σ components on the two possible directions of the polarizer are expressed by four functions. These functions can be derived [11] by considering the angular dependence of a radiating dipole: the π components are equivalent to a dipole oscillating along the electric field, while the σ components are equivalent to a dipole rotating in the perpendicular plane. The resulting functions are

$$\begin{aligned} &f_{1,\pi}(\cos\theta)=3\cos^2\theta \ , \\ &f_{2,\pi}(\cos\theta)=f_{1,\sigma}(\cos\theta)=\tfrac{3}{2}(1-\cos^2\theta) \ , \\ &f_{2,\sigma}(\cos\theta)=\tfrac{3}{4}(1+\cos^2\theta) \ . \end{aligned} \tag{3}$$

With this formalism the problem is reduced to the construction of the distribution function for the quasistatic electric fields $W(\mathcal{E},\cos\theta)$ from the distribution functions for the isotropic and the anisotropic electric fields in the plasma.

Turbulent electric fields in plasmas have often been assumed to follow Rayleigh (Gaussian-like) distribution functions [11,14,30,31]. Such distributions are obtained if the turbulence can be viewed as a superposition of a very large number of statistically independent fluctuations [31]. In a situation of a fully developed turbulence in the plasma a three-dimensional Gaussian function is then appropriate. However, as Bekefi and Deutch [30] have pointed out, such a distribution represents a very advanced stage of the turbulence, and a one-dimensional Gaussian distribution may be more appropriate for a turbulence that results from growing waves along a preferred direction. A distribution function similar to a one-dimensional Gaussian distribution has also been attained in numerical simulations [32]. Since our data support a one-dimensional assumption for the anisotropic fields we use such a distribution, i.e.,

$$W(\mathcal{E}_T)d\mathcal{E}_T=(\pi\langle\mathcal{E}_T^2\rangle)^{-1/2}\exp\left[-\frac{\mathcal{E}_T^2}{\langle\mathcal{E}_T^2\rangle}\right]d\mathcal{E}_T \ . \tag{4}$$

As for the particle fields, the Holtzmark distribution function is a reasonable approximation for our plasma since the number of particles in a Debye sphere is large (>1000).

Although the distribution function of the particle fields is isotropic, it cannot be assumed to result from statistically independent one-dimensional distribution functions for each of the components of these fields (see below). The total distribution function was constructed by numerically integrating over the directions and magnitudes of the isotropic field, weighted by the Holtzmark distribution, convoluted with the one-dimensional Gaussian distribution assumed for the turbulent fields.

B. Gaussian approximation

If the probability distribution functions of the components of the electric field [$W(\mathcal{E}_x)$, $W(\mathcal{E}_y)$, and $W(\mathcal{E}_z)$] are statistically independent and if, furthermore, the total distribution function is isotropic, then these distribution functions must necessarily be Gaussian functions. This can be seen from the combination of two mathematical conditions expressing the statistical independence of the different components:

$$W(\mathcal{E}=(\mathcal{E}_x,\mathcal{E}_y,\mathcal{E}_z))=W(\mathcal{E}_x)W(\mathcal{E}_y)W(\mathcal{E}_z) \tag{5}$$

and the isotropy of the total function

$$W(\mathcal{E})=f(\mathcal{E}_x^2+\mathcal{E}_y^2+\mathcal{E}_z^2) \ . \tag{6}$$

Since the true distribution of electric fields in the plasma is not a Gaussian it follows that the probability distribution functions of the components of the isotropic particle electric fields in the plasma are not statistically independent. This fact makes the construction explained above of the total distribution function $W(\mathcal{E},\cos\theta)$ quite cumbersome and time consuming. However, the Holtzmark probability function can be approximated by a three-dimensional Rayleigh function for fields smaller than about twice the Holtzmark field. Approximating both the particle fields and the turbulent fields by Rayleigh distribution functions allows the axially symmetric distribution function $W(\mathcal{E},\cos\theta)$ to be readily obtained, thus simplifying the calculations considerably, although failing to give the correct asymptotic behavior. With this approximation, the distribution function of the electric fields perpendicular to the symmetry axis is determined only by the particle fields and is given by

$$W_1(\mathcal{E}_\perp)d\mathcal{E}_\perp=2(\langle\mathcal{E}_\perp^2\rangle)^{-1}\exp\left[-\frac{\mathcal{E}_\perp^2}{\langle\mathcal{E}_\perp^2\rangle}\right]\times\mathcal{E}_\perp d\mathcal{E}_\perp \ . \tag{7}$$

In the direction of the symmetry axis, the probability distribution function is determined by the convolution of the two Gaussian functions that describe the particle and the turbulent electric fields. The resulting function is

$$W_2(\mathcal{E}_\parallel)d\mathcal{E}_\parallel=(\pi\langle\mathcal{E}_\parallel^2\rangle)^{-1/2}\times\exp\left[-\frac{\mathcal{E}_\parallel^2}{\langle\mathcal{E}_\parallel^2\rangle}\right]\times d\mathcal{E}_\parallel \ , \tag{8}$$

where $\langle\mathcal{E}_\parallel^2\rangle=\langle\mathcal{E}_T^2\rangle+\langle\mathcal{E}_P^2\rangle$, $\langle\mathcal{E}_T^2\rangle$, and $\langle\mathcal{E}_P^2\rangle$ are the widths of the distribution functions of the turbulent and the particle fields, respectively, and $\langle\mathcal{E}_P^2\rangle=\frac{1}{2}\langle\mathcal{E}_\perp^2\rangle$. The distribution function for the total field is

$$W(\mathcal{E},\cos\theta)d\mathcal{E}\,d(\cos\theta)=\left[\frac{4}{\pi\langle\mathcal{E}_{\parallel}^2\rangle}\right]^{1/2}\frac{\mathcal{E}^2}{\langle\mathcal{E}_{\perp}^2\rangle}\exp\left\{-\frac{\mathcal{E}^2}{\langle\mathcal{E}_{\perp}^2\rangle}-\cos^2\theta\left[\frac{\mathcal{E}^2}{\langle\mathcal{E}_{\parallel}^2\rangle}-\frac{\mathcal{E}^2}{\langle\mathcal{E}_{\perp}^2\rangle}\right]\right\}d\mathcal{E}\,d(\cos\theta)\ . \tag{9}$$

With this axially symmetric distribution function the calculation of the resulting profiles is straightforward and relatively fast. Comparing the linewidths and width differences obtained using the Gaussian approximation to those obtained using the full calculation of the distribution showed the former are satisfactorily correct over a wide range of parameters if $\langle\mathcal{E}_P^2\rangle^{1/2}$ is chosen to be $\simeq 1.3F_0$, where F_0 is the Holtzmark field. This method proved to be useful in the repeated calculations performed to study the effects of the various parameters on the line profiles, although the final results were compared to the results of the full calculation.

Using the detailed calculations we checked the dependence of the width difference on the amplitude of the anisotropic 1D electric fields. The width difference $\Delta\omega$ was found to be $\Delta\omega\alpha(\langle\mathcal{E}_T^2\rangle+A^2)^{1/2}-A$, where A is approximately the Holtzmark field F_0. This functional form is similar to that obtained for the width of a convolution of two Gaussian profiles, and it is consistent with the validity of the Gaussian approximation discussed above. If the anisotropic electric fields dominate, the broadening $\Delta\omega$ is linear with the field amplitude, as expected from the linearity of the Stark effect for the hydrogen lines. When the isotropic fields dominate, the broadening $\Delta\omega$ varies nearly quadratically with $\langle\mathcal{E}_T^2\rangle^{1/2}$.

In summary, the Gaussian approximation was found to be useful in the analysis of the FWHM of the hydrogen line profiles, although it should not be used for the analysis of the line wings. To the best of our knowledge, this approximation has never been used before for the particle fields in the plasma, although a Gaussian distribution has been often assumed for the description of the turbulent fields.

C. Results

The data analysis described above was used to determine three parameters: the velocities of the hydrogen atoms, the amplitude of the turbulent electric fields in the x direction ($\langle\mathcal{E}_T^2\rangle^{1/2}$), and the plasma density. Each of these three parameters affects to a different extent various aspects of the H_α and H_β profiles observed for the different lines of sight and polarizations, and they were used to reconstruct the profiles self-consistently.

Our analysis of the H_α profiles observed for polarizations perpendicular to the anisotropic fields showed that these profiles are dominated by Doppler broadening, and are relatively insensitive to the electric fields or to the plasma density. The insensitivity of the H_α profiles to these parameters results from the dominance of the Doppler-broadened unshifted component for these polarizations. As an example, we use the width (FWHM) of 2.3 Å obtained for the y polarization in the z measurements at the regions $x=0$–0.5 mm for the time $t=50$–70 ns. Assuming that this width results only from Doppler broadening gives a temperature of 21 eV. Adding broadenings by electric fields with an amplitude of 15 kV/cm and a plasma density of 2×10^{15} cm^{-3} (which are maximum values for our plasma, see below) reduces the hydrogen temperature inferred to $\simeq 14$ eV, corresponding to Doppler broadening of 1.9 Å. The narrower profiles of 1.54–1.81 Å given in Table I for the z polarization ($x=0.5$–1 mm) correspond to a temperature of 9–13 eV if the entire width is attributed to Doppler broadening, or 6–8 eV if electric fields and a plasma density with the maximum values are assumed.

The anisotropic electric fields are mainly obtained from the differences between the widths for the various polarizations observed for both H_α and H_β. Let us address again the results obtained in the z measurements using the 2-cm-long anode, averaged over $t=50$–70 ns for $x=0$–0.5 mm. The measured H_β widths for the x and y polarizations, respectively, were 4.2 and 3.6 Å with a difference of 0.61 ± 0.17 Å, and the H_α widths were 2.6 and 2.3 Å (a difference of 0.30 ± 0.10). A difference of 0.6 Å for H_β is obtained for $\langle\mathcal{E}_T^2\rangle^{1/2}\simeq 7.5$–$11$ kV/cm for any plasma density in the range of 5×10^{14}–2×10^{15} cm^{-3}. Similarly, for the same density range, a width difference of 0.3 Å between the H_α widths is obtained for $\langle\mathcal{E}_T^2\rangle^{1/2}\simeq 6$–$8.5$ kV/cm.

The plasma density is now determined mainly by the observed H_β linewidths. The observed H_β widths are similar to those previously used to obtain the plasma density, giving $n_e\simeq 2.3\times10^{15}$. Accounting for the effect of turbulent fields on the line broadening gives a plasma density that is about twice lower than that obtained by considering only the effect of the particle fields. The determined density for the above results is $(1.3\pm0.3)\times10^{15}$ cm^{-3}.

Both H_α and H_β widths for this time and plasma region were thus found to be consistent with an electric-field distribution resulting from plasma ions at a density of 1.3×10^{15} cm^{-3} and a one-dimensional Gaussian fluctuating-field distribution with $\langle\mathcal{E}_T^2\rangle^{1/2}$ of $\simeq 8$ kV/cm. A Doppler broadening corresponding to a hydrogen temperature of 15 eV was found to best fit the data for both H_α and H_β profiles. The uncertainty in the determination of each of these parameters is about $\pm25\%$.

The correction for the turbulent field effect in the electron density determination was larger for certain times and distances from the anode surface. For example, width differences for the x and z polarizations that are especially large, 0.9–1.0 Å, were found for H_α for $t=80$–90 ns and $x=0.5$–1.0 mm, see Table I. For such a large width difference to occur the Gaussian one-dimensional distribution must have $\langle\mathcal{E}_T^2\rangle^{1/2}$ larger than 10 kV/cm for a reasonable plasma density. Using such values for $\langle\mathcal{E}_T^2\rangle^{1/2}$, a plasma density as low as 5×10^{14} cm^{-3} is required for an agreement between the calculated H_α and H_β profiles and the observed ones. Using a higher plasma density of 10^{15} cm^{-3}, although it allows us to obtain an agreement for the H_α profile (by assuming

$\langle \mathcal{E}_T^2 \rangle^{1/2} = 15$ kV/cm), yields an H_β width for the x polarization larger than observed. This conclusion is insensitive to the Doppler broadening assumed.

The drop in time of the differences between the widths for the orthogonal polarizations, as shown in Figs. 6 and 7, was observed in all measurements for both H_α and H_β. As noted in the previous section, the width differences are expected to vary linearly with the field in the weak-field limit and quadratically in the strong-field limit. Thus the time dependence of the fields inferred in our analysis resembles that of the width differences as shown in Fig. 9 for the data given in Fig. 6(a). In this calculation a density $\simeq 1\times 10^{15}$ cm^{-3} and a Doppler broadening corresponding to a hydrogen temperature of 7–14 eV were found to be consistent with measured widths for each time instant. The uncertainty in the amplitude of the electric fields shown in Fig. 9, ± 3 kV/cm, is dominated by the measurement errors shown in Fig. 6(a) and the uncertainty in the determination of the plasma density. The field amplitude appears to have a maximum value of about 10 kV/cm at $t = 50$–60 ns, followed by a decay. For $t = 120$ ns the H_α line was slightly wider in the direction perpendicular to the x direction, so that our assumption of a one-dimensional fluctuating-field distribution in the x direction cannot explain the data. For this point the data was analyzed assuming a one-dimensional distribution in the y direction, giving $\langle \mathcal{E}_y^2 \rangle^{1/2}$ shown in Fig. 9.

An interesting observation is that for our range of plasma densities a Doppler broadening corresponding to a hydrogen temperature of a few eV is essential for significant differences in the H_α widths for the orthogonal polarizations. For a Doppler broadening corresponding to ≤ 1 eV the effect of the anisotropic fields is significantly only at the wings of the H_α profile, and the FWHM of the line is determined by the broadening of the unshifted central component that is not affected by quasistatic electric fields. Consider, for example, a plasma density of 10^{15} cm^{-3} and a hydrogen temperature of 3 eV, corresponding to a Doppler FWHM of 0.9 Å. For these parameters an additional 1D field distribution of $\langle \mathcal{E}_T^2 \rangle^{1/2} = 10$ kV/cm would result in widths of 1.1 and 1.4 Å for the two orthogonal polarizations, i.e., a width difference of 0.3 Å. On the other hand, if a hydrogen temperature of only 1 eV is assumed (FWHM = 0.5 Å), the respective widths for these parameters would be 0.68 and 0.74 Å, giving a width difference of only 0.06 Å. We note, however, that for densities much lower than the densities presently considered the central component of the H_α profile might almost disappear for the polarization parallel to the fluctuating fields and significant differences between the widths for various polarizations occur even in the absence of a Doppler broadening.

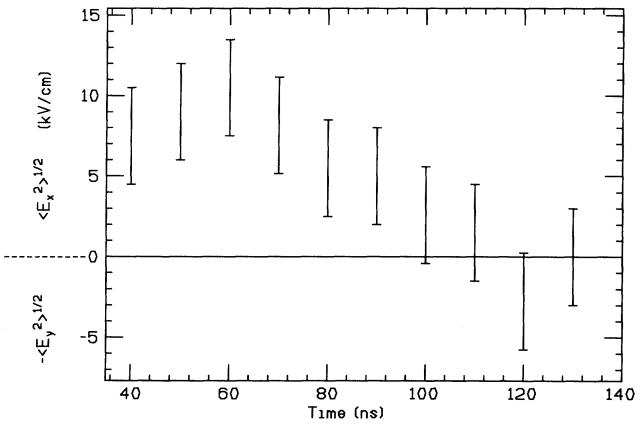

FIG. 9. Mean amplitude of the electric field $\langle \mathcal{E}_x^2 \rangle^{1/2}$ inferred as a function of time using the data shown in Fig. 6(a). Here, the plasma density was assumed to be 10^{15} cm^{-3} and the Doppler broadening was chosen to make the calculated widths and the measured ones agree for each time instant. For the data point at 120 ns, the width for the x polarization was smaller than for the y polarization, which is inconsistent with the assumption of a one-dimensional field in the x direction. For this point, the same analysis is used to obtain a field in the y direction with an amplitude $\langle \mathcal{E}_y^2 \rangle^{1/2}$, as shown in the figure.

V. DISCUSSION

Polarization spectroscopy was used to determine the amplitude of the anisotropic electric fields in the plasma, the time dependence of the amplitude, and the main direction of the fields throughout the 100-ns pulse. The present measurements do not yield information on the frequencies of these anisotropic fields. However, we expect that these fields oscillate in time and/or in space in the x direction. Otherwise, they would have accelerated the plasma ions to kinetic energies much higher than those observed, $\simeq 25$ eV for the C III ions [6]. Static electric fields of a few kV/cm would have doubled this energy over a distance of a few tens of micrometers in about 1 ns. Therefore, the observed anisotropic fields must oscillate with spatial and/or temporal periods smaller than these values.

Note, that in principle, the motion of the hydrogen atoms across the magnetic field could cause the hydrogen lines to be Stark split even in the absence of electric fields in the laboratory frame. However, for our hydrogen velocities the field $E = VB/c$ is at least $10\times$ smaller than the electric fields considered.

In a separate presentation, Litwin, Sarid, and Maron [22] suggested that the ion flow observed in the plasma in the x direction leads to an instability that can grow during the pulse. The predictions of this model are consistent with the direction, the size, and the time dependence of the observed fields. Thus, this model suggests that the field amplitude should decrease with the ion drift velocity. Indeed, the electric fields observed were found to decrease in time during the pulse (see Fig. 8), similar to the ion flow velocity that is shown in Ref. [6].

Investigating the fluctuating electric fields in a plasma is important not only for studying the plasma stability, but also for the determination of the plasma parameters. In our plasma, the fluctuating fields were found to be larger or comparable in amplitude to the Holtzmark field ($\simeq 4$ kV/cm) that is a measure of the particle isotropic fields in the plasma. In our previous determination of the electron density from the hydrogen line Stark broadening [6] we ignored the effect of the collective electric fields on

the line broadening and therefore overestimated the electron density. The effect of the collective fields in the present study led us to lower the electron density inferred for our plasma from 2.2×10^{15} cm^{-3} to 1.3×10^{15} cm^{-3}. For plasmas in which the collective fields are larger compared with the particle fields, neglecting the effect of collective fields on the line broadening may lead to even larger errors in the determination of the electron density.

In most pulsed-power plasmas the atomic level populations do not reach a steady state and, therefore, the determination of the electron temperature for observed line intensities requires knowledge of the electron density. In our previous study [8], we used time-dependent observations and detailed time-dependent collisional-radiative calculations to determine the electron temperature in our nonequilibrium anode plasma, based on our electron density determined from line broadening. A value of 5–8 eV was obtained. The use of lower electron density for our plasma, as borne out by the present study, suggests the inference of higher electron temperature from the line intensities observed in Ref. [8]. Our calculations show that for an electron density $\simeq1.3\times10^{15}$ cm^{-3} the electron temperature should be corrected to 10 ± 3 eV.

A few observations, such as the magnetic-field penetration into the plasma and the plasma expansion against the magnetic field suggested that the plasma conductivity is anomalous, significantly lower than the classical conductivity [6,7]. The higher electron temperature here suggested means that the classical conductivity is higher than previously assumed, i.e., the discrepancy between the anomalous conductivity inferred and the classical one is even larger. In the previous studies [6,8] the plasma pressure gradient was used to estimate the plasma expansion rate and the electron joule heating. However, since the plasma pressure is dominated by the more energetic ions, the use of a higher temperature for the electrons does not affect those estimates. Finally, the association of the fluctuating electric fields presently observed with the anomalous plasma conductivity inferred requires further investigation. We believe that such measurements can be useful in studying turbulence in various ns duration plasmas.

ACKNOWLEDGMENTS

The authors are grateful to C. Litwin, A. E. Blaugrund, H. R. Griem, and E. A. Oks for their stimulating comments. The authors are indebted to Pesach Meiri for his skilled technical help.

*Present address: Department of Physics, University of California, San Diego, La Jolla, California 92093.

[1] V. N. Tsytovich, *Theory of Turbulent Plasma* (Consultants Bureau, New York, 1977).
[2] B. B. Kadomtsev, *Plasma Turbulence* (Academic, New York, 1965).
[3] P. L. Similon and R. N. Sudan, Annu. Rev. Fluid Mech. **22**, 317 (1990).
[4] J. C. Callen, B. A. Carreras, and R. D. Stambaugh, Phys. Today **45** (1), 34 (1992).
[5] *Turbulence and Anomalous Transport in Magnetized Plasmas,* Proceedings of the International Workshop at "Institut d'Etudes Scientifiques de Cargèse," Corse du Sud, France, 1986, edited by D. Gresillon and M. A. Dubois (Editions de Physique, Les Ulis, France, 1987).
[6] Y. Maron, E. Sarid, O. Zahavi, L. Perelmutter, and M. Sarfaty, Phys. Rev. A **39**, 5842 (1989).
[7] Y. Maron, E. Sarid, E. Nahshoni, and O. Zahavi, Phys. Rev. A **39**, 5856 (1989).
[8] Y. Maron, M. Sarfaty, L. Perelmutter, O. Zahavi, M. E. Foord, and E. Sarid, Phys. Rev. A **40**, 3240 (1989).
[9] T. Nee and H. R. Griem, Phys. Rev. A **14**, 1853 (1976).
[10] P. C. Liewer, Nuclear Fusion **25**, 543 (1985).
[11] G. V. Sholin and E. A. Oks, Dokl. Akad. Nauk. SSSR **209**, 1318 (1973) [Sov. Phys. Dokl. **18**, 254 (1973)].
[12] E. K. Zavoiskii, Yu. G. Kalinin, V. A. Skoryupin, V. V. Shapkin, and G. V. Sholin, Pis'ma Zh. Eksp. Teor. Fiz. **13**, 19 (1971) [JETP Lett. **13**, 12 (1971)].
[13] A. B. Berezin, L. V. Dubovi, and B. V. Ljublin, Zh. Tekh. Fiz. **41**, 2323 (1971) [Sov. Phys. Tech. Phys. **16**, 1844 (1972)].
[14] M. V. Babykin, A. I. Zhuzhunashvili, E. A. Oks, V. V. Shapkin, and G. V. Sholin, Zh. Eksp. Teor. Fiz. **65**, 175 (1973) [Sov. Phys. JETP **38**, 86 (1974)].
[15] Ya. Volkov, V. G. Dyatlov, and N. I. Mitina, Zh. Tekh. Fiz. **44**, 1448 (1974) [Sov. Phys. Tech. Phys. **19**, 905 (1975)].
[16] A. B. Berezin, B. V. Ljublin, and D. G. Yakovlev, Zh. Tekh. Fiz. **54**, 1897 (1984) [Sov. Phys. Tech. Phys. **29**, 1116 (1984)].
[17] V. A. Rantsev-Kartinov, Fiz. Plazmy **13**, 387 (1987) [Sov. J. Plasma Phys. **13**, 217 (1987)].
[18] P. Bakshi and G. Kalman, Solar Phys. **43**, 307 (1976).
[19] H. R. Griem, *Spectral Line Broadening by Plasmas* (Academic, New York, 1974).
[20] G. Bekefi, C. Deutch, and B. Yaakobi, in *Principles of Laser Plasmas,* edited by G. Bekefi (Wiley, New York, 1976).
[21] E. A. Oks and G. V. Sholin, Zh. Tekh. Fiz. **46**, 254 (1976) [Sov. Phys. Tech. Phys. **21**, 144 (1976)].
[22] C. Litwin, E. Sarid, and Y. Maron, Bull. Am. Phys. Soc. **35**, 2120 (1990).
[23] R. Pal and D. Hammer, Phys. Rev. Lett. **50**, 732 (1983).
[24] Y. Kawano, N. Yumino, K. Masugata, and K. Yatsui, Laser Particle Beams **7**, 277 (1989).
[25] Y. Maron, L. Perelmutter, E. Sarid, M. E. Foord, and M. Sarfaty, Phys. Rev. A **41**, 1074 (1990).
[26] L. Perelmutter, G. Davara, and Y. Maron, *Proceedings of the XIV International Symposium on Discharges and Electrical Insulation in Vacuum, Santa Fe, New Mexico, 1990,* edited by R. W. Stinnett, p. 318.
[27] H. R. Griem, *Plasma Spectrscopy* (McGraw-Hill, New York, 1964).
[28] D. H. Oza, R. L. Greene, and D. E. Kelleher, Phys. Rev. A **38**, 2544 (1988).
[29] D. H. Oza, R. L. Greene, and D. E. Kelleher, Phys. Rev. A **37**, 531 (1988).
[30] G. Bekefi and C. Deutch, Comm. Plasma Phys. Contr. Fusion **2**, 89 (1976).
[31] C. Deutsch and G. Bekefi, Phys. Rev. A **14**, 854 (1976).
[32] H. H. Klein and N. A. Krall, Phys. Rev. A **8**, 881 (1972).